Preparation of an environmentally friendly lead adsorbent. A contribution to the rational design of heavy metal adsorbents

Ezequiel Rossi [a, b], Jhon Alejandro Ávila Ramírez [a, b], María Inés Errea [a*]

[a] Instituto Tecnológico de Buenos Aires (ITBA), Departamento de Ingeniería Química. Av. Eduardo Madero 399 (CP 1106ACD), Buenos Aires, Argentina. Tel/fax: 0054 11 37544693. ezrossi@itba.edu.ar; javila@itba.edu.ar

[b] Consejo Nacional de Investigaciones Científicas y Técnicas (CONICET), Argentina.

*Corresponding author: Tel/fax: 0054-11-3754-4694

E-mail address: merrea@itba.edu.ar

Graphical Abstract

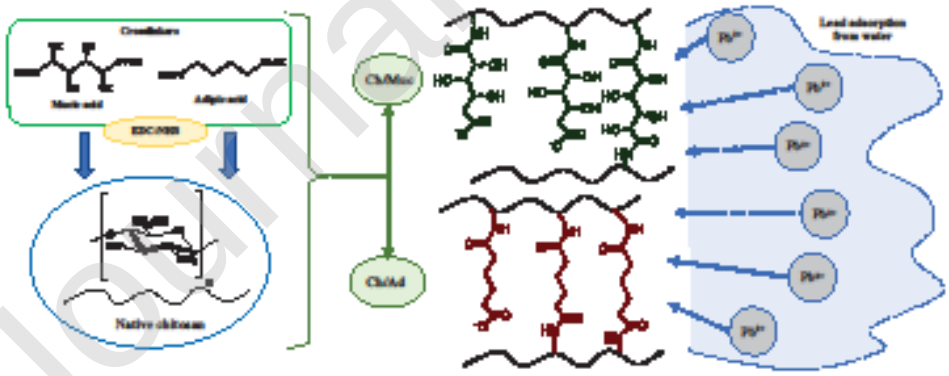

Highlights

- In highly regioselective reactions *N*-substituted chitosan derivatives were achieved
- Mucic and adipic acid were used as crosslinkers
- Crosslinking degree were influenced by the crosslinker structure
- The new materials exhibited good lead adsorption capacity

Abstract

This work described the preparation and characterization of water insoluble chitosan derivatives as lead adsorbents. In highly regioselective reactions, *N*-substituted crosslinked chitosan derivatives were obtained by crosslinking native chitosan with mucic and adipic acid (a polyhydroxylated and a non-functionalized diacid of the same length chains). The crosslinking degree of the chitosan modified with adipic acid was significantly higher than that crosslinked with mucic acid (0.446 and 0.316, respectively), while the degree of substitution was almost the same (approximately 80%). Lead adsorption isotherms were constructed at different temperatures and adjusted to well-known models, obtaining the best fit to the experimental data with Langmuir model. The lead adsorption capacity of new materials was greater than many of the adsorbents described in literature (76.3 and 69.7 mg g^{-1} for chitosan modified with mucic and adipic acid, respectively). Moreover, thermodynamic parameters were calculated, and results showed that the lead adsorption on the derivatives was spontaneous, exothermic, and governed by chemical interaction. Besides, kinetic studies were performed and adjusted to well-known models. The pseudo-second order kinetic equation was the one that most appropriately described the lead adsorption on the new materials. Results were consistent

with the strong electrostatic attraction established between the lead cations and the free carboxylate groups of the derivatives.

Keywords: chitosan, crosslinking, mucic acid, lead adsorption

1. Introduction

For long enough, it has been well known that human activities have a negative impact in water quality [1-4]. Among the water pollutants, heavy metals are of special concern because, in addition to their non-biodegradability, they are toxic even at such low concentration that do not alter the organoleptic properties of the water, therefore consumers do not know the risk of drinking that water [5]. In particular, lead (Pb) is a potent neurotoxin and its ions (Pb II) may cause critical diseases in human beings, including cancer, as mentioned in previous works [6-9]. Due to the health hazard of consuming lead-contaminated water, the World Health Organization (WHO) has set the maximum permissible lead concentration in drinking water at 0.01 mg L^{-1} [10, 11].

For all the reasons mentioned above, intensive work is being done on the development of materials and technologies for the treatment of lead-contaminated water [12, 13]. Among the different methodologies proposed for lead removal, adsorption using adsorbents from natural, renewable, and environmentally friendly raw materials have attracted the attention of the scientific community because of their cost-effectiveness, their sustainable long-term availability and their harmlessness to the ecosystem. In particular, cellulose and chitin, as they are the most abundant polysaccharides on Earth, have aroused special interest. Therefore, in recent times a significative number of lead

adsorption studies carried out over modified cellulose, cellulose based materials or chitin derivatives, were reported [6, 14-18].

Chitosan is obtained by partial deacetylation of chitin ((1→4)-2-acetamino-2-deoxy-β-D-glucopyranose). Due to the basic character of the amino group, native chitosan is completely soluble in aqueous medium at pH below 5, which limits its use as metal adsorbent [19-21]. Therefore, many efforts are being made towards achieving insoluble materials in acidic environment from chitosan. Substitution involving the C-6 hydroxyl group and/or the C-2 amino group, crosslinking reactions, as well as grafting of polymeric chains, like polyacrylonitrile, methyl polyacrylate, polyvinyl acetate, polyethylene glycol, polyvinylpyridine, among others, were reported [22-24].

Unfortunately, modifications sometimes incorporate into the chitosan structure molecules that could represent a risk to health or the environment. This is, for example, the case of methyl polyacrylate [25] or vinyl acetate [26]. Therefore, it is worth facing the challenge of developing metal adsorbents using only abundant and environmentally friendly materials coming from renewable biomass.

Considering the above discussion, this work proposes the crosslinking of chitosan chains through amide bonds using mucic acid, a nontoxic and environmentally friendly polyhydroxylated dicarboxylic acid, coming from renewable biomass. In order to better understand the factors involved in the adsorption process of the new chitosan derivative and hence improve the design of new heavy metals adsorbent materials, the crosslinking reaction was also carried out with adipic acid, a non-functionalized dicarboxylic acid of the same chain length as mucic acid. The comparison between both derivatives could show how hydroxyl groups affect the cross-link reaction and the properties of the final product. The new materials were subjected to chemical, physical, and morphological studies.

Besides, lead adsorption studies were also carried also out. Adsorption isotherm at different temperatures were constructed, thermodynamic parameters were calculated, and the adsorption mechanism was discussed. Furthermore, the effects of operational parameters (pH, and contact time) on the adsorption capacity were also investigated.

2. Materials and Methods

2.1.Chemicals and reagents

Medium molecular weight chitosan was purchased from Sigma (Sigma-Aldrich 448877) and characterized in the same way that their derivatives. Adipic acid, mucic acid, *N*-hydroxysuccinimide (NHS), *N*-ethyl-*N'*-(3-dimethylaminopropyl) carbodiimide hydrochloride (EDC) were all reagent grade and purchased from Sigma-Aldrich. Sodium hydrogen carbonate ($NaHCO_3$) (Merck), hydrochloric acid (Merck) and sodium hydroxide (Merck) were all analytical grade and used as received without further purification.

2.2.Preparation of chitosan derivatives

2.2.1. Preparation of Chitosan modified with adipic acid (Ch/Ad)

To a solution of adipic acid (122 mg) in 20 mL of water, chitosan (350 mg, 1.68 mmol of deacetylated units) was added. Then, pH was adjusted to 6.5 by addition of NaOH (0.1 M) and the resulted solution was cooled in an ice bath.

EDC (1.6 g, 8.4 mmol) was added to a solution of NHS (965 mg, 8.4 mmol) in water (about 3 mL), previously cooled in an ice bath. The mixture was added to the chitosan and adipic acid solution with energetic mechanical stirring.

The reaction mixture was left with mechanical stirring in an ice bath until gelation was observed (about 8 h) and then it was kept at 4ºC for 16 h. Finally, a 10% NaOH aqueous solution was added to quench the reaction (50 mL) [27], the product was separated by centrifugation (5000 rpm, 15 min) and then washed sequentially with HCl (0.1 M, x3), NaOH (10%, x3), and finally water until neutral pH was reached. The product obtained as a gel was lyophilized to give 458 mg of a white powder (Ch/Ad) [27, 28].

2.2.2. Chitosan modification with mucic acid (Ch/Muc)

In this case, chitosan (350 mg, 1.68 mmol of deacetylated units) was dissolved in 16.8 mL of 0.1 M HCl aqueous solution (molar ratio NH_2: HCl 1:1). In another flask, mucic acid (176.3 mg, 0.84 mmol) and $NaHCO_3$ (141.1 mg, 1.68 mmol) were dissolved in the minimum volume of water (about 2 mL) and the mixture was added to the chitosan solution. The pH was adjusted to 6.5 by addition of NaOH (0.1 M), the solution was cooled in an ice bath, and then the synthesis proceeded as described for adipic acid.

The product was obtained as a gel and lyophilized to give 510 mg of a white powder (Ch/Muc).

2.3.Characterization Methods

Fourier transform infrared spectra (*FT*-IR) of native chitosan and its derivatives before and after lead adsorption were acquired on a Thermo Scientific Nicolet 6700 spectrometer in transmission mode. The samples were mixed with KBr (Grade *FT*-IR 99+%, Thermo Spectra-Tech) at 1:100 ratio (sample:KBr) and an aliquot were pressed into a disc of 5 mm using a Hand Press accessory PIKE Technologies. Samples were scanned 32 times at a spectral resolution of 4 cm^{-1} in the range of 400 to 4000 cm^{-1}.

In order to determine its acetylation degree, native chitosan (50 mg) was titrated conductometrically as described elsewhere [29].

The substitution degree of chitosan derivatives was determined by heterogeneous conductometric titration. Lyophilized chitosan derivatives (300 mg) were suspended in 10 mL of HCl aqueous solution (0.1 M) with vigorous stirring and then titrated with NaOH aqueous solution (0.1 M). Conductivity values were registered each 0.05 mL using a Hanna Instruments HI-2300 conductometer.

Quantitative solubility assays of chitosan derivatives were performed in water, HCl aqueous solution (0.1 M) and NaOH aqueous solution (0.1 M). 100 mg of Ch/Muc or Ch/Ad were suspended in each solvent (10 mL) with magnetic stirring for 24 h at room temperature. Then, the solid was separated by centrifugation (5000 rpm, 15 min), lyophilized, and finally weighed.

Qualitative solubility assays were also carried out. Particularly, DMSO and DMF were screened by adding successive amounts of each solvent to a known mass of chitosan derivatives with continuous stirring.

The isoelectric point of the chitosan derivatives was determined by measuring the Zeta potential as function of pH using a Zetasizer Nano ZS coupled with MPT-2 autotitrator (Malvern Panalytical). Chitosan derivatives (1 mg) were dispersed in 0.01 M HCl solution (25 mL) and the pH was varying by the addition of 1 M NaOH solution [30, 31].

X-ray diffraction patterns were obtained using a Philips PW1730/10 automated wide-angle powder X-ray diffractometer operated at 40 kV and 20 mA, with Cu/Kα radiation (λ = 0.154 nm). Diffractograms were recorded in a 2θ angle range of 5-40° with a scan rate of 0.02° s^{-1} and a step size of 0.02º.

The morphology of native chitosan and its derivatives was studied with a scanning electron microscope Carl Zeiss Evo 10 with field emission gun operated at 3 kV. Samples

were deposited on microscope glasses in their swollen gel form and dried at 40°C for 5 minutes. All samples were coated with a thin layer of gold using an ion sputter coater.

2.4.Lead adsorption experiments

Aqueous solutions of Pb (II) were prepared from solid $Pb(NO_3)_2$ p.a.(Merck) with ultrapure water (18MΩ quality). Lead concentration was determined on an air-acetylene flame type atomic absorption spectrometer (FAAS) (Model iCE 3000, Thermo Scientific). Pb (II) standard solutions for the FAAS analyses were prepared from 1000 mg L^{-1} Pb standard solution (Merck). All lead adsorption studies were performed in duplicate.

The adsorption isotherms were constructed by adding a fixed amount of native chitosan, Ch/Muc or Ch/Ad (25 mg) to 25 mL of lead solution (50–150 mg L^{-1}) at pH 7. Then, two parallel experiments were carried out stirring the mixtures at 400 rpm for 3 h at 25 or 50°C. After filtration, lead concentration was determined by FAAS [6].

The effect of pH on the adsorption of lead was studied in a pH range of 2.5–7.0 at 25°C. 25 mL of an aqueous lead solution (150 mg L^{-1}) were shaken in presence of 25 mg of Ch/Muc or Ch/Ad at 400 rpm for 3 h. The pH of the solutions was adjusted using NaOH (0.01 M) or HCl (0.01 M). After filtration, lead concentration was determined by FAAS [6].

Besides, the adsorption kinetics were also studied. Ch/Muc or Ch/Ad (25 mg) were suspended in 50 mL of lead solution (100 mg L^{-1}) at pH 7 and the mixtures were stirred at 400 rpm at different temperatures (25 and 50°C). Samples were taken from each suspension at different times and lead concentration was determined by FAAS [6].

Finally, regeneration studies were carried out with aqueous HCl solution (6 mM, pH 2.2). Ch/Muc or Ch/Ad (25 mg) were suspended in 50 mL of the HCl solution and the mixtures were stirred at 400 rpm for 3 h. After filtration, lead concentration was

determined by FAAS. Then, the adsorbents were conditioned with an NaOH aqueous solution (10 mM, 25 mL) and washed with water until pH 7 prior to use again to study their reuse. The procedure was repeated 3 times.

3. Results and discussion

3.1.Analysis of reaction regioselectivity - determination of the substitution degree of the products

When chitosan is subjected to acylation reactions, the substitution could be an *O*-acylation at the C-3 and/or C-6 positions of the D-glucosamine unit or an *N*-acylation on its -NH_2 group. However, probably due to the greater reactivity of the amino group and the less steric hindrance of the *O*-6 with respect to the *O*-3, acylation on the C-3 position was never reported [32, 33].

Therefore, when chitosan reacts with an activated dicarboxylic acid, substitution is expected to be an *O*-acylation at C-6 position of the D-glucosamine unit or an *N*-acylation on its amino group (Fig. 1). Besides, the crosslinking degree is not predictable and, in the cases in which the reaction involved just one of the carboxylic groups of the diacid, the other group would remain as carboxylate after the alkaline treatment involved in the work up of the reaction (structures II and IV in Fig. 1) [27, 28, 34].

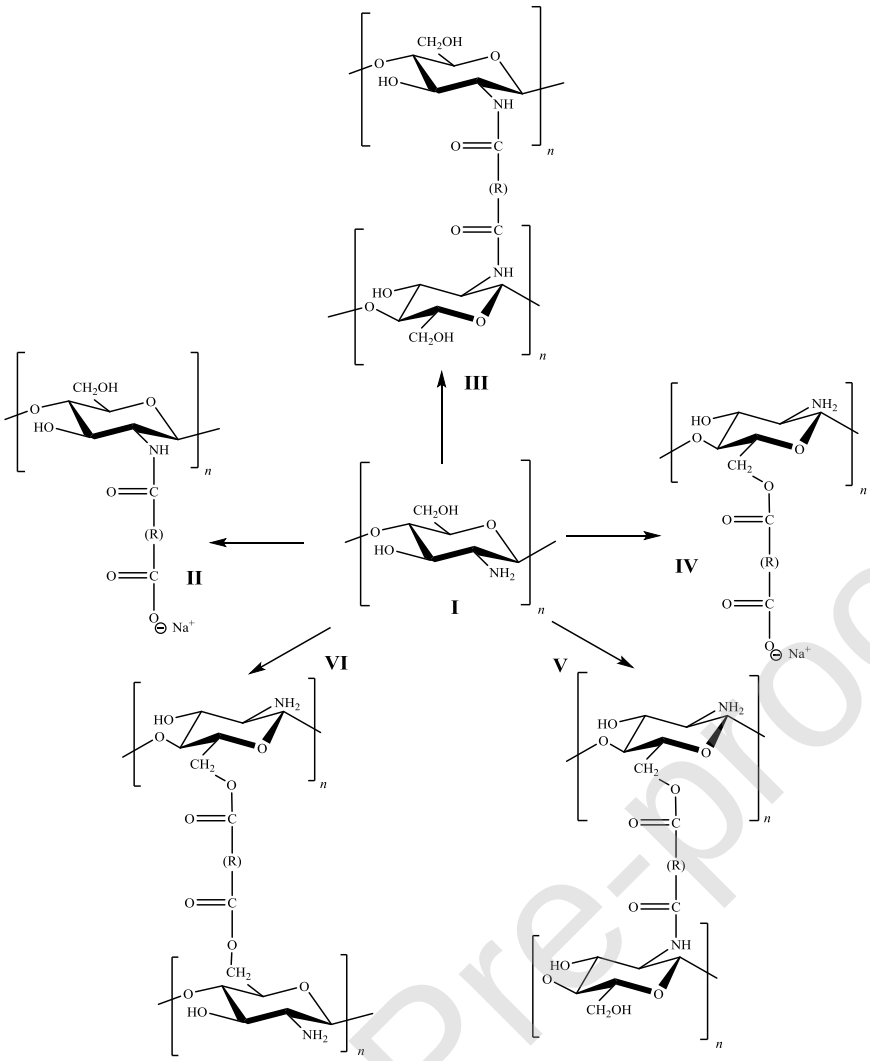

Figure 1. Expected structural units that could be found in the chitosan derivatives.

Considering the above discussion, acylation reactions could lead to complex mixtures difficult to analyze, and it is even harder when the products result insoluble in all media. This might be the reason why, on such derivatives, studies to discern substitution or crosslinking degree are not usually reported.

In order to know the substitution pattern of the new derivatives, *FT*-IR analyses and conductimetric titration studies were carried out. Figure 2 compares the *FT*-IR spectra of the native chitosan and its derivatives. In the spectra of chitosan derivatives an increment in the relative intensity of the signals at 1650 and 1560 cm^{-1} with respect to

that of the native chitosan was clearly observed. Since those signals correspond to the stretching carbonyl vibration and the N-H bending vibration of secondaries amides, the increment in their intensity must be related with an increment on the proportion of amide groups in the samples after the reaction. Besides, no evidence of ester formation was observed, since the expected signal at about 1730 cm^{-1} corresponding to the stretching vibration of the ester carbonyl group was not observed in the spectra.

These results were consistent with high regioselective reactions towards the amino groups and allowed to dismiss the presence of significant proportion of *O*-acylated structural units in the chitosan derivatives (structures IV, V and VI in Fig. 1). Unfortunately, the stretching vibration of carboxylate groups, if present, will appear at about 1600 cm^{-1}, overlapped with amide bands. Thus, by *FT*-IR there was not possible either to dismiss or confirm the presence of carboxylate groups (structure II in Fig. 1) in the samples.

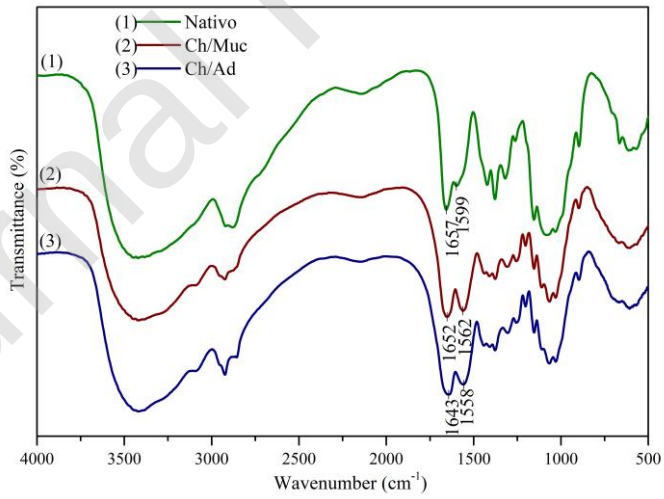

Figure 2. FT-IR spectra of native chitosan, Ch/Muc and Ch/Ad.

In summary, the structural indeterminacy that remained after the *FT*-IR analyses was either the presence or absence of the structures I, II and III (Fig. 1) in the samples. In order to solve this indetermination, as well as to calculate the molar proportion of each unit, conductometric titration studies were carried out. The conductometric titration curves of native chitosan and its derivatives are shown in Supplementary Data (Fig. S1-S3) and were obtained by plotting electrical conductivity as a function of volume of NaOH solution added to the analyzed solution. In all cases, the straight-line equations were determined by linear regression and the equivalence points were calculated from the intersection of the lines. Unlike the native chitosan, titration of the derivatives was carried out in heterogeneous systems, but all samples were measured with the same experimental set-up and the results were processed in the same way.

In the titration curve of native chitosan, three linear portions with different slopes (see Fig. S1 in Supplementary Data) were observed. The deacetylation degree was determined using both equivalence points and Equation 1, where *%DD* is the percentage of deacetylated D-glucosamine units, *203* and *161* are the weight of the acetylated and deacetylated units respectively (*g mol*$^{-1}$), *[NaOH]* is the concentration of sodium hydroxide (*mol L*$^{-1}$), V_1 and V_2 are the volumes of each equivalence points (*L*) and *m* is the mass of chitosan (*g*). The deacetylation degree (*81%, SD 1.8%*) was consistent with that reported by the suppliers of the material.

$$\%DD = \frac{203 \cdot (V_2 - V_1) \cdot [\mathrm{NaOH}]}{m + (203 - 161) \cdot (V_2 - V_1) \cdot [\mathrm{NaOH}]} \cdot 100\% \qquad \text{Eq. 1}$$

In the titration curves of the chitosan derivatives four linear portions with different slopes were observed, confirming that the derivates had one more functional group with

acid-basic behavior, with respect to the native polysaccharide (see Fig. S2 and S3 in Supplementary Data). This result was consistent with the presence of free carboxylic acid groups in the derivatives.

Considering the above discussion, the structures that must be present in the derivatives are summarized in Figure 3.

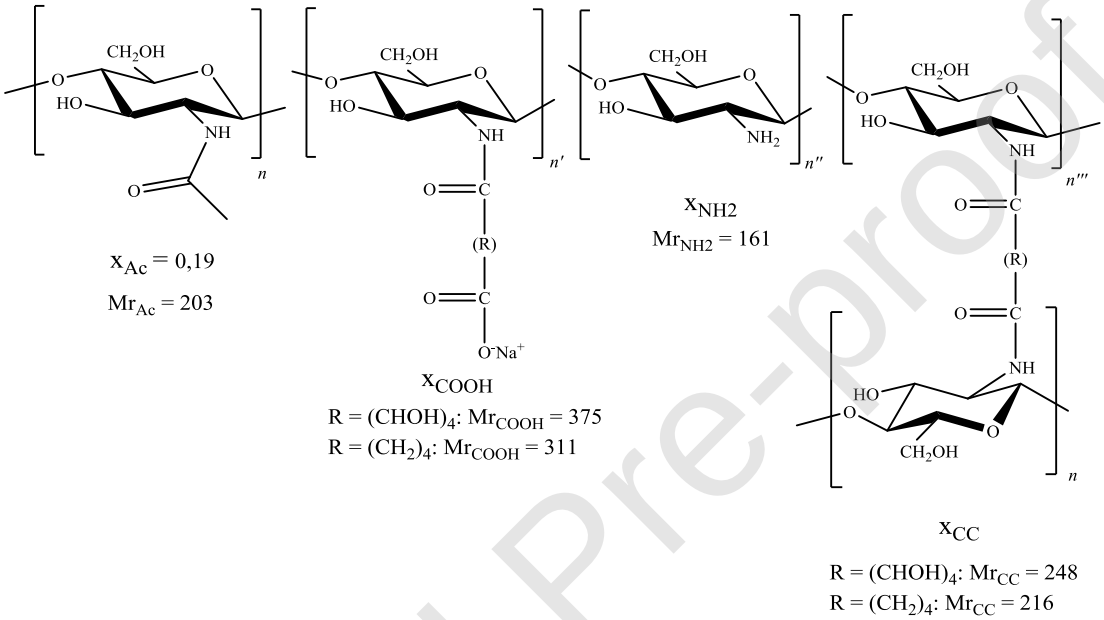

Figure 3. Structural units present in the derivatives.

It was assumed that the percentage of acetylated units in the derivatives was the same as in the native chitosan. The percentages of the others structural units were calculated using Equations 2, 3 and 4, where ΔV_1 is the NaOH volume consumed between first and second equivalence point (L), ΔV_2 is the NaOH volume consumed between second and third equivalence point (L), *[NaOH]* is the molar concentration of NaOH solution, m is the mass of the chitosan derivative (g), x are the number fraction and Mr are the molecular weight of each structural unit ($g\ mol^{-1}$), respectively, and $\overline{Mr}$ is the average molecular weight of the structural units ($g\ mol^{-1}$). Results are shown in Table 1.

$$x_{COOH} \cdot \frac{m}{\overline{Mr}} = \Delta V_1 \cdot [\text{NaOH}] \quad \text{Eq. 2}$$

$$x_{NH2} \cdot \frac{m}{\overline{Mr}} = \Delta V_2 \cdot [\text{NaOH}] \quad \text{Eq. 3}$$

$$\overline{Mr} = Mr_{COOH} \cdot x_{COOH} + Mr_{NH2} \cdot x_{NH2} + Mr_{CC} \cdot x_{CC} + Mr_{Ac} \cdot x_{Ac} \quad \text{Eq. 4}$$

Chitosan derivatives	x_{COOH} (%)	x_{NH2} (%)	x_{CC} (%)	x_{Ac} (%)
Ch/Muc	30.5 (SD 0.9)	18.8 (SD 0.7)	31.6 (SD 1.2)	19 (SD 1.8)
Ch/Ad	19.3 (SD 1.8)	17.1 (SD 1.5)	44.6 (SD 2.3)	19 (SD 1.8)

Table 1. Percentages of chitosan derivatives' structural units.

The substitution achieved on the free amino groups was almost the same for Ch/Muc and Ch/Ad (77% and 79%, respectively). On the other hand, the crosslinking degree was, in both cases, higher than previously reported in literature for similar systems [30, 31], and significantly lower in Ch/Muc respect to Ch/Ad (0.316 and 0.446, respectively).

The significantly lesser crosslinking achieved in Ch/Muc respect to the Ch/Ad could be a consequence of hydrogen bonding interaction between the mucic acid hydroxyl groups and chitosan chains. Such interaction would cause a decrease in the mucic chain flexibility, turning difficult the required approach between its second carboxyl group and another chitosan chain to form a new amide bond.

3.2.Solubility assays

Quantitative solubility assays of the chitosan derivatives were performed suspending each sample in distilled water, HCl aqueous solution (0.1 M), and NaOH

aqueous solution (0.1 M). No significant loss of mass was detected after 24 h in any of the cases, which indicated that the products were insoluble in all the media studied, as it was expected for highly crosslinked materials [35].

Qualitative solubility assays were also carried out in different solvents (DMSO and DMF), with identical results.

3.3.Measurements of Zeta potential as function of pH

Figure 4 shows the curves obtained by measured the Z-potential of both derivatives as a function of pH. At low pH values, since both ammonium and carboxyl groups were protonated, the Z-potential was positive. When pH increased, carboxyl groups began to deprotonate, achieving the isoelectric point when the amount of carboxylate groups equaled to that of ammonium groups. Then, the Z-potential became negative.

These results were consistent with those obtained by *FT*-IR and conductometric titration. Since the number of free carboxyl group of Ch/Muc is greater than that of Ch/Ad, the isoelectric point of this derivative was lower than that of Ch/Ad (4.5 and 5.2, respectively).

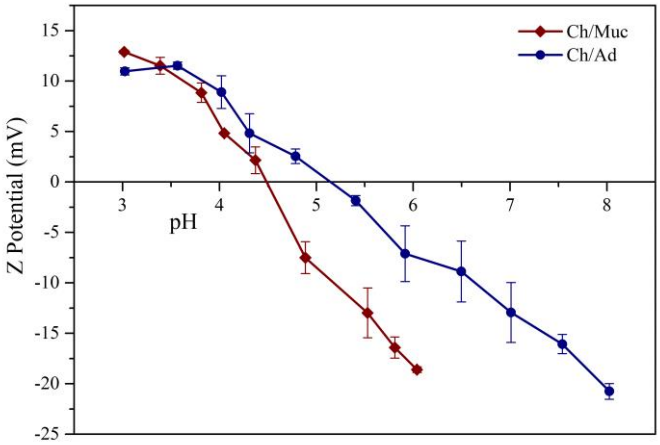

Figure 4. Measurements of Z-potential of both derivatives as a function of pH.

3.4.X-ray diffraction studies

The diffractograms of lyophilized native chitosan and its derivatives are shown in Figure 5. Two diffraction peaks were observed in the diffractogram of the native chitosan, one of greater intensity at $2\theta = 20^{o}$ and the other at 11^{o}, assigned to crystalline forms II and I, respectively. When the chitosan was modified, the crystallinity was completely lost, observing in the diffractograms of both modified products only the characteristic pattern of the amorphous phase [36].

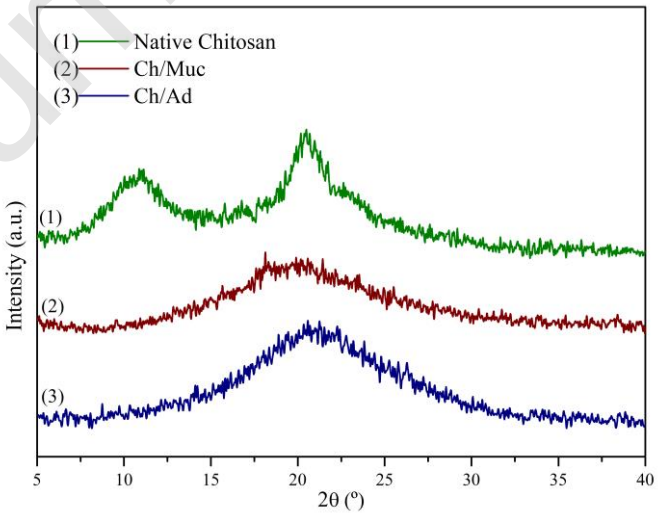

Figure 5. XRD patterns of native chitosan, Ch/Muc and Ch/Ad.

3.5.Morphological studies

Comparative morphological studies of native chitosan and its derivatives were performed by scanning electron microscopy (SEM) (Fig. 6). For the analysis of the samples, they were first hydrated by suspension in water and then dried at 40ºC. In the micrographs of the native chitosan, a flat and smooth surface without roughness, was observed, while in the derivatives a rougher surface was observed, compatible with the loss of crystallinity determined by XRD [36].

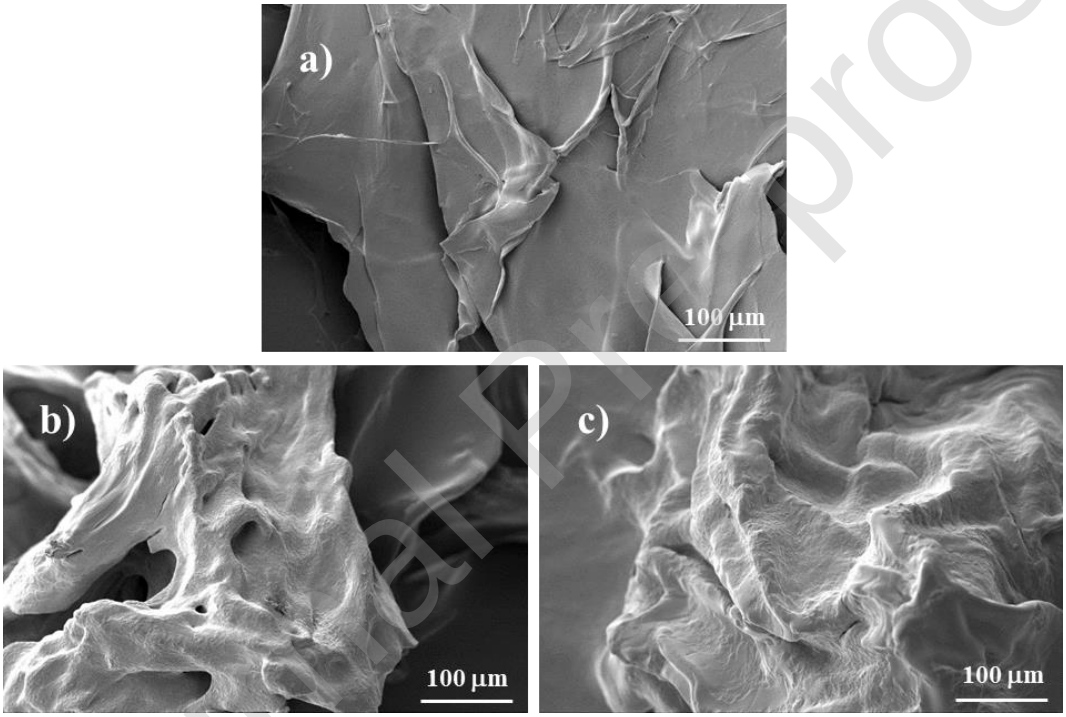

Figure 6. SEM images of native chitosan (a), Ch/Muc (b) and Ch/Ad (c).

3.6.Lead Adsorption Studies

3.6.1. Adsorption Isotherms

Equilibrium data, commonly known as sorption isotherms, are basic requirements for the design of adsorption systems. They are obtained by plotting the amount of lead retained on the adsorbent as a function of its concentration in the supernatant, under

equilibrium conditions at constant temperature. In this work, the adsorption isotherms were measured at two different temperatures (25 and 50°C).

Taking into account that native chitosan is soluble in acidic medium and at pH above 7 an insoluble lead hydroxide precipitates [6, 37], the working pH was set at 7 for the construction of all adsorption isotherms.

Different well-known models of sorption isotherms (Langmuir, Freundlich, Dubinin-Radushkevich and Frumkin) were fitted to experimental isotherm data. All the parameters of the models were obtained by nonlinear fit using Origin Pro 9.0.0 software, and the adjusted determination coefficient (R_{adj}^2), the root-mean-square error (*RMSE*) and the Akaike's information criterion (*AIC*) are shown in Table 2. As it can be seen, the Langmuir equation gives the best fit of the collected data [38].

Figure 7 shows the experimental data and the curves obtained by the Langmuir model for Ch/Muc and Ch/Ad, and compares them with that of native chitosan. In addition, the separation factor R_L indicates the type of the isotherm to be either unfavorable ($R_L > 1$), linear ($R_L = 1$), favorable ($0 < R_L < 1$) or irreversible ($R_L = 0$). In this case, the values of R_L factor were always between 0 and 1 for any value of initial concentration (C_0), indicating that adsorption of lead onto the chitosans is favorable [39-41].

As it can be seen in Figure 7, chemical modifications greatly improved the adsorption capacity of chitosan, and it is noteworthy that the new materials showed higher lead adsorption capacity than many adsorbents described in literature [42, 43]. The improvement on lead adsorption capacity of Ch/Ad and Ch/Muc with respect to native chitosan can be attributed to two main factors: ionic interactions between the carboxylate groups and lead cations; and the disruption of the crystalline structure of chitosan

confirmed by the XRD studies, that would facilitate the interaction between lead and chitosan chains.

The higher lead adsorption capacity of Ch/Muc respect to Ch/Ad (76.3 and 69.7 mg g^{-1}, respectively) is consistent with the higher number of free carboxylate groups in Ch/Muc respect to Ch/Ad (30.5 % and 19.3 %, respectively).

The decrease in the adsorption capacity of the chitosans as the temperature increased was in accordance with an exothermic process, as it will be confirmed by the calculations of the thermodynamic parameters in the next Section.

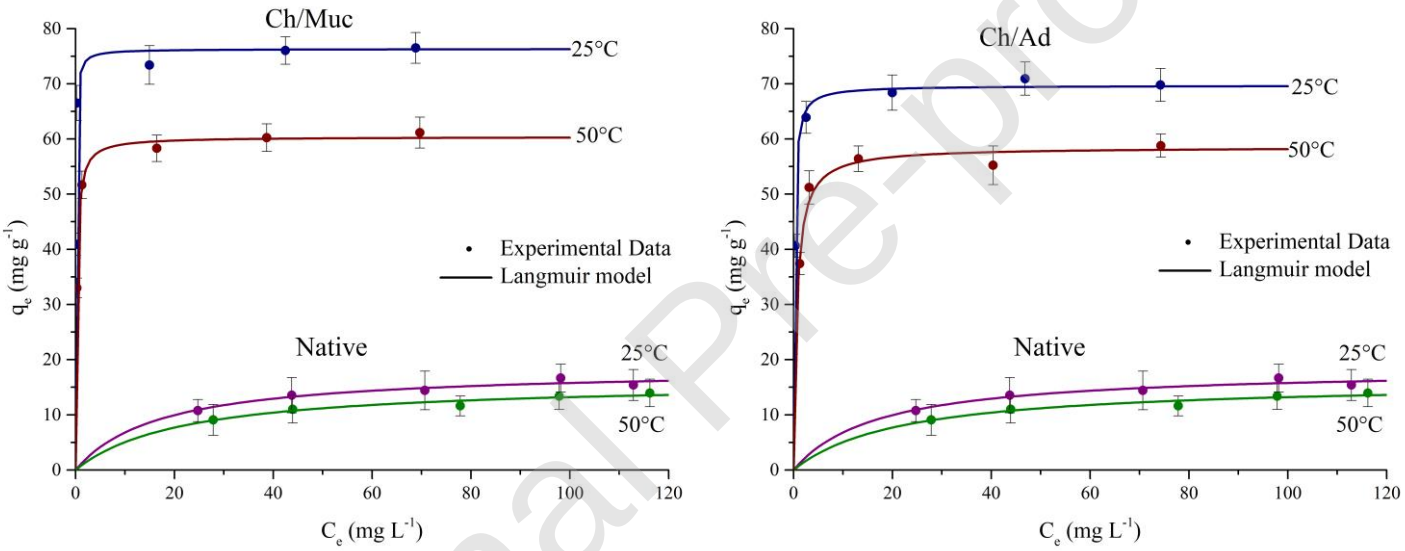

Figure 7. Adsorption isotherm of lead on native chitosan, Ch/Muc and Ch/Ad.

Model	Equation	Parameters	Native		Ch/Ad		Ch/Muc		
			25°C	50°C	25°C	50°C	25°C	50°C	
Langmuir	$q_e = \frac{q_{max} \cdot K_L \cdot C_e}{1 + K_L \cdot C_e}$ $R_L = \frac{1}{1 + K_L \cdot C_0}$	q_{max}	18.5 (SD 1.06)	16.1 (SD 1.0)	69.7 (SD 0.7)	58.5 (SD 1.4)	76.3 (SD 3.3)	60.4 (SD 0.5)	mg g^{-1}
		K_L	0.058 (SD 0.015)	0.046 (SD 0.012)	5.9 (SD 0.47)	1.59 (SD 0.29)	16.8 (SD 4.8)	4.52 (SD 0.28)	L mg^{-1}
		R_{adj}^2	0.8934	0.8972	0.9898	0.9305	0.8555	0.9938	
		RMSE	0.72	0.62	1.27	2.24	5.7	0.93	
		AIC	24.2	22.7	29.8	35.5	44.8	26.7	
Freundlich	$q_e = k_{Fre} \cdot C_e^{\,n}$	k_{Fre}	5.2 (SD 1.2)	3.6 (SD 0.65)	52.5 (SD 4.0)	42.3 (SD 4.0)	60.5 (SD 5.1)	44.0 (SD 3.6)	mg g^{-1}
		n	0.24 (SD 0.053)	0.28 (0.041)	0.079 (SD 0.023)	0.081 (SD 0.03)	0.062 (SD 0.025)	0.087 (SD 0.025)	
		R_{adj}^2	0.847	0.9254	0.7664	0.6383	0.5914	0.7712	
		RMSE	0.87	0.53	6.1	5.1	9.56	5.6	
		AIC	26.0	21.1	45.7	43.8	50.02	44.7	
Dubinin–Radushkevich	$q_e = q_{D-R} \cdot \exp(-k_{D-R} \cdot \varepsilon^2)$ $\varepsilon = RT \ln(1 + C_e^{-1})$ $E = \frac{1}{\sqrt{2k_{D-R}}}$	q_{D-R}	15.9 (SD 0.53)	13.5 (SD 0.57)	68.7 (SD 1.23)	56.8 (SD 0.8)	76.3 (SD 3.3)	59.2 (SD 1.16)	mg g^{-1}
		k_{D-R}	4.3 10^{-5} (SD 9.3 10^{-6})	4.7 10^{-5} (SD 1.2 10^{-5})	3.1 10^{-8} (SD 3.7 10^{-9})	1.7 10^{-7} (SD 1.7 10^{-8})	1.3 10^{-8} (SD 3.1 10^{-9})	2.44 10^{-8} (SD 4.1 10^{-9})	mol^2 J^{-2}
		E	108	103	4001	1713	6089	3810	J mol^{-1}
		R_{adj}^2	0.8607	0.8034	0.9629	0.9694	0.8523	0.9649	
		RMSE	0.83	0.86	2.4	1.5	5.7	2.2	
		AIC	25.6	26.0	36.3	31.4	44.9	35.3	
Frumkin	$\frac{\theta}{1-\theta} \cdot \exp(-2a\theta) = K_{Fru} \cdot C_e$ $\theta = \frac{q_e}{q_{max}}$	a	1.2 (SD 0.95)	0.68 (SD 0.47)	4.8 (SD 15)	-0.08 (SD 4.3)	3.5 (SD 7.4)	4.1 (SD 8.7)	
		K_{Fru}	0.009 (SD 0.014)	0.016 (SD 0.012)	0.002 (SD 0.049)	0.77 (SD 6.4)	0.01 (SD 0.14)	0.005 (SD 0.09)	L mg^{-1}
		R_{adj}^2	0.477	0.8714	-0.822	0.7469	0.602	0.4418	
		RMSE	26.5	13.2	42.5	15.9	18.8	21.9	
		AIC	60.2	53.2	65.0	55.1	56.8	58.3	

Table 2. Adsorption isotherm model parameters (means and standard deviations (SD)) (q_e: equilibrium adsorption capacity; C_e: concentration of the balance solution; C_0: initial concentration of the solution).

3.6.2. Thermodynamic parameters

The equilibrium constant (K_c) is related to $\Delta G°$ by Equation 6 and to $\Delta H°$ and $\Delta S°$ by Equation 7, where T is the temperature in Kelvin and R is the gas constant. $\Delta H°$ and $\Delta S°$ were obtained from the slope and intercept of linear Van't Hoff plots of *ln Kc* versus T^{-1} [6, 44]. The results are shown in Table 3.

The equilibrium constants (K_c) were calculated from those obtained by Langmuir model (K_L) [45, 46] using Equation 5, where Ar_{Pb} is the atomic mass of lead (207.2 g mol^{-1}), $[Pb^{+2}]^0$ is the standard concentration ($1\ mol\ L^{-1}$) and γ is the coefficient of activity that was considered equal to *1* because the measurements were made on dilute solutions [47, 48].

$$K_c = \frac{1000 \cdot K_L \cdot Ar_{Pb} \cdot [\mathrm{Pb}^{+2}]^0}{\gamma} \qquad \text{Eq. 5}$$

$$\ln K_c = \frac{-\Delta G°}{RT} \qquad \text{Eq. 6}$$

$$\ln K_c = \frac{\Delta S°}{R} - \frac{\Delta H°}{RT} \qquad \text{Eq. 7}$$

Chitosan	T (K)	K_L (L mg^{-1})	K_c	$\Delta G°$ (kJ mol^{-1})	$\Delta H°$ (kJ mol^{-1})	$\Delta S°$ (J mol^{-1} K^{-1})
Native	298	0.058	12045	-23.4 (SD 0.6)	-8.0 (SD 12)	51.2 (SD 38.7)
	323	0.046	9469	-24.6 (SD 0.7)		
Ch/Muc	298	16.8	3471965	-37.4 (SD 0.7)	-43.8 (SD 9.9)	-21.3 (SD 30.7)
	323	4.5	937232	-36.9 (SD 0.2)		
Ch/Ad	298	5.87	1216264	-34.8 (SD 0.2)	-43.8 (SD 6.7)	-30.1 (SD 22.1)
	323	1.58	327376	-34.1 (SD 0.5)		

Table 3. Thermodynamics parameters for the adsorption of lead in native chitosan and its derivatives (means and standard deviations (SD)).

The negative values of $\Delta G°$ indicate the spontaneous nature of the adsorption process of lead onto the chitosans. In addition, the negative value of $\Delta S°$ in the chitosan derivatives, which indicates a decrease in the randomness of the interface, is consistent with the loss of translational freedom of the lead cations when they are retained in the active sites of the adsorbent by the electrostatic forces exerted by the carboxylate groups introduced into the chitosan structure in the derivatization process. In the case of native chitosan, the entropy variation was positive, which implies that lead does not lose translational freedom, which is consistent with a process governed by physical adsorption [6]. These results are consistent with the high value of the enthalpy modulus determined for the chitosan derivatives ($|\Delta H°| > 40\ kJ\ mol^{-1}$), according with an adsorption mechanism governed by chemical interactions, and the low value determined for the native chitosan which is in accordance with a process of physical adsorption [39]. No evidence of additional interactions between lead cations and chitosan chains was obtained in any of the cases, since the *FT*-IR spectra of Ch/Muc, Ch/Ad and native chitosan did not show significant differences with respect to those of the same samples saturated with lead (see Fig. S4 in Supplementary Data). Besides, the decrease in the lead adsorption capacity of chitosans when the temperature increased from 25°C to 50°C (Fig. 7) is in agreement with an exothermic process, as confirmed by the negative value of enthalpy variation.

3.6.3. Effect of pH

The strong pH dependence of lead adsorption on chitosan derivatives is shown in Figure 8. These results were in agreement with those obtained by conductometric and Zeta potential titrations. Given that at low pH values both amino and carboxyl groups are protonated, the lead cations could not be retained on the material by ionic interaction. As

the pH increases, the carboxyl groups begin to deprotonate, and the maximum lead adsorption capacity of the materials were observed at the maximum pH assayed. As previously mentioned, the maximum working pH was 7, because above this value a water-insoluble lead hydroxide precipitates.

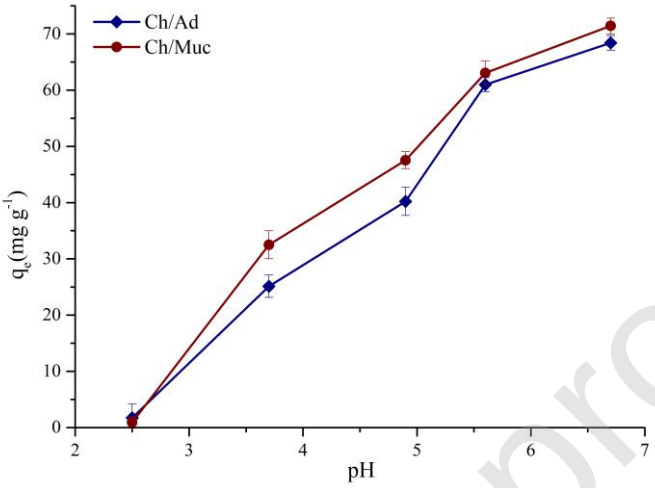

Figure 8. Effect of pH on the lead adsorption capacity of chitosan derivatives.

3.6.4. Adsorption kinetics studies

The studies were performed at 25 and 50°C and in both cases the equilibrium was reached in less than 45 min (Fig. 9). Besides, a decrease in the capture rate was observed as the active sites of the chitosan derivatives were being occupied and, upon saturation of the adsorbent, the curves reached a plateau.

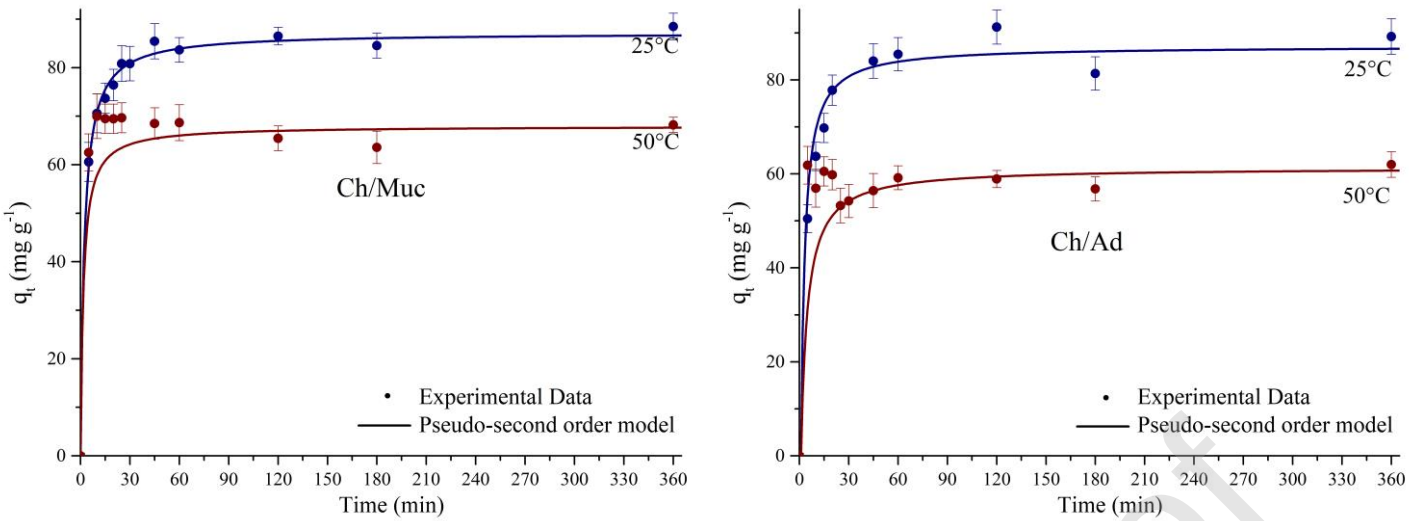

Figure 9. Amount adsorbed of Pb^{+2} on chitosan derivatives at different times and temperatures.

In order to infer the controlling mechanism of the adsorption process, experimental data were adjusted by pseudo-first order and pseudo-second order models (Eq. 7 and 8, respectively), where k_1 (min^{-1}) and k_2 (g mg^{-1} min^{-1}) are the kinetics rate constants, q_e (mg g^{-1}) is the adsorption capacity and q_t (mg g^{-1}) is the adsorption uptake at time t (min) [49-51].

$$q_t = q_{max} \cdot (1 - \exp(-k_1 \cdot t)) \quad \text{Eq. 8}$$

$$q_t = \frac{q_{max}^{\ 2} \cdot k_2 \cdot t}{1 + q_{max} \cdot k_2 \cdot t} \quad \text{Eq. 9}$$

All parameters obtained for both models, as well as the adjusted determination coefficient (R_{adj}^2), the root-mean-square error (*RMSE*) and the Akaike's information criterion (*AIC*), are shown in Table 4.

The best fit was achieved using the pseudo-second-order kinetic equation which suggests, as it is well known, that the adsorption mechanism is kinetically controlled mainly by adsorbent-adsorbate interactions, which is consistent with an adsorption mechanism governed by the strong electrostatic interactions established between the lead cations and the free carboxylate groups [6]. Figure 8 shows the good concordance between the experimental data and those calculated by pseudo-second-order kinetic equation.

		Ch/Ad		Ch/Muc	
Model	Parameters	25°C	50°C	25°C	50°C
Pseudo-first order model	k_1 (min^{-1})	0.14 (SD 0.014)	0.08 (SD 0.01)	0.22 (SD 0.03)	0.27 (SD 0.04)
	q_e (mg g^{-1})	86 (SD 1.7)	59.7 (SD 0.9)	83 (SD 1.3)	66.1 (SD 1.2)
	R_{adj}^2	0.9744	0.9902	0.9716	0.9849
	RMSE	4.3	1.9	3.9	2.9
	AIC	39.1	20.4	42.2	26.5
Pseudo-second order model	k_2 (g mg^{-1} min^{-1})	0.0029 (SD 0.0003)	0.0043 (SD 0.0009)	0.0050 (SD 0.0004)	0.0084 (SD 0.0017)
	q_e (mg g^{-1})	89.7 (SD 1.3)	61.3 (SD 0.9)	87.2 (SD 0.6)	68.0 (SD 1.2)
	R_{adj}^2	0.9883	0.9939	0.9960	0.9896
	RMSE	2.9	1.5	1.5	2.4
	AIC	30.5	16.2	16.9	23.6

Table 4. Comparison of the adsorption kinetic models (means and standard deviations (SD)).

3.6.5. Regeneration studies

Given that the possibility of reusing the adsorbent is one of the critical factors to consider in order to propose these materials for an industrial application, Ch/Muc and Ch/Ad was regenerated using HCl 6 mM (pH 2.2) and three adsorption/desorption cycles were performed. As it can be seen in Figure 10, the regeneration process was successful

and no significant changes in the adsorption capacity of the samples were observed after being exposed to the regeneration cycles.

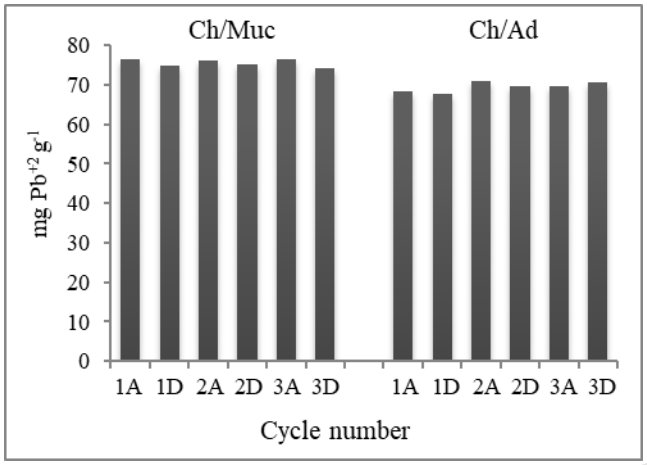

Figure 11. Adsorption capacity and desorbed lead amount with HCl (6 mM) for Ch/Muc and Ch/Ad though the three cycles of adsorption (A) and desorption (D).

4. Conclusions

In this work, in highly regioselective reactions *N*-substituted crosslinked chitosan derivatives were achieved, and the crosslinking degree was markedly influenced by the crosslinker structure. When the rection was carried out with a polyhydroxylated diacid, the crosslinking degree of the derivative was significantly lower than that achieved when the crosslinker was a non-functionalized diacid of the same chain length (0.316 and 0.446, respectively). Difference found in the crosslinking degree between the derivatives could be attributed to the interaction via hydrogen bond of the polyhydroxylated chain of the mucic acid with those of chitosan, making it difficult for the second carboxyl group of the hydroxylated acid to approach another chitosan chain to form a new amide bond. As a consequence, a less crosslinked product was obtained.

Besides, as substitution degree in the modified chitosan was not influenced by the crosslinker structure, lesser crosslinking led to a higher number of free carboxyl group in the derivate which was consistent with the observed increase in the lead adsorption capacity of Ch/Muc respect to Ch/Ad (76.3 and 69.7 mg g^{-1}, respectively), mainly attributed to ionic interaction between the lead ions and the free carboxylate groups. It is important to note that, although the lead adsorption capacity of Ch/Muc was greater than that of Ch/Ad, both derivatives exhibited a higher adsorption capacity than many of the adsorbents described in literature [42, 43]. Furthermore, regeneration studies were successful turning these new materials as promising economic and environmentally friendly lead adsorbents.

Results reported herein are encouraging enough to carry out a systematic study of the reaction conditions to produce Ch/Muc with a crosslinking degree high enough to guarantee the insolubility of the material, and the largest number of free carboxylate groups to maximize the amount of electrostatic interactions between lead cations and carboxylate groups. These ionic interactions are responsible for the adsorption of lead on the chitosan derivatives, as it was shown in the current study. Besides, it is also worth deepening the study of hydrogen binding forming groups as chitosan crosslinker as a valuable tool to modulate the properties of the final products.

CRediT author statement

Ezequiel Rossi: Methodology, Investigation, Formal Analysis, Writing-original draft, Visualization. **Jhon Alejandro Ávila Ramírez:** Investigation, Visualization. **María Inés Errea:** Conceptualization, Funding Acquisition, Project Administration, Writing-original draft, Writing-Review & Editing.

Declaration of interests

The authors declare that they have no known competing financial interests or personal relationships that could have appeared to influence the work reported in this paper.

Acknowledgments

The authors acknowledge Instituto Tecnológico de Buenos Aires for financial support. Ezequiel Rossi and Jhon Alejandro Ávila Ramírez have fellowships from CONICET. The authors acknowledge to Ana Scarella (Sworn Translator) and Juan Maffi for the English revision of the manuscript.

5. References

[1] Kass, A., I. Gavrieli, Y. Yechieli, A. Vengosh, and A. Starinsky, *The impact of freshwater and wastewater irrigation on the chemistry of shallow groundwater: a case study from the Israeli Coastal Aquifer*. J Hydrol, 300 (2005) 314-331. https://doi.org/10.1016/j.jhydrol.2004.06.013

[2] Al Yaqout, A.F., *Assessment and analysis of industrial liquid waste and sludge disposal at unlined landfill sites in arid climate.* Waste Manage., 23 (2003) 817-824. https://doi.org/10.1016/S0956-053X(03)00036-9

[3] Khan, N.A., et al., *Occurrence, Sources and Conventional Treatment Techniques for various antibiotics present in hospital wastewaters: A critical review.* TrAC, Trends Anal. Chem., (2020) 115921. https://doi.org/10.1016/j.trac.2020.115921

[4] Khan, N.A., et al., *Recent trends in disposal and treatment technologies of emerging-pollutants- A critical review.* TrAC, Trends Anal. Chem., 122 (2020) 115744. https://doi.org/10.1016/j.trac.2019.115744

[5] Sharma, S. and A. Bhattacharya, *Drinking water contamination and treatment techniques.* Appl. Water Sci., 7 (2017) 1043-1067. 10.1007/s13201-016-0455-7

[6] Rossi, E., Ú.M. Rojo, P. Cerrutti, M.L. Foresti, and M.I. Errea, *Carboxymethylated bacterial cellulose: An environmentally friendly adsorbent for lead removal from water.* J. Environ. Chem. Eng., 6 (2018) 6844-6852. https://doi.org/10.1016/j.jece.2018.10.055

[7] Liu, B., H. Qin, B. Zhang, T. Shi, and Y. Cui, *Enhanced oxidative stress by lead toxicity retards cell survival in primary thyroid cells.* Int. J. Clin. Exp. Med., 10 (2017) 4590-4597.

[8] Schober, S.E., L.B. Mirel, B.I. Graubard, D.J. Brody, and K.M. Flegal, *Blood Lead Levels and Death from All Causes, Cardiovascular Disease, and Cancer: Results from the NHANES III Mortality Study.* Environ. Health Perspect., 114 (2006) 1538-1541. doi:10.1289/ehp.9123

[9] Muhammad, S., Y. Muhammad, K. Muti-ur-Rehman, A.A. Anjum, and E.-u.-H. Syed, *Effects of experimental lead toxicity on hematology and biochemical parameters in Lohi sheep.* Int. J. Agric. Biol., 19 (2017) 1409-1413. DOI: 10.17957/IJAB/15.0425

[10] Mohan, D., H. Kumar, A. Sarswat, M. Alexandre-Franco, and C.U. Pittman, *Cadmium and lead remediation using magnetic oak wood and oak bark fast pyrolysis bio-chars.* Chem. Eng. J., 236 (2014) 513-528. https://doi.org/10.1016/j.cej.2013.09.057

[11] Rajput, S., L.P. Singh, C.U. Pittman, and D. Mohan, *Lead (Pb2+) and copper (Cu2+) remediation from water using superparamagnetic maghemite (γ-Fe2O3) nanoparticles synthesized by Flame Spray Pyrolysis (FSP).* JCIS, 492 (2017) 176-190. https://doi.org/10.1016/j.jcis.2016.11.095

[12] Xu, M. and G. McKay, *Removal of Heavy Metals, Lead, Cadmium, and Zinc, Using Adsorption Processes by Cost-Effective Adsorbents*, in *Adsorption Processes for Water Treatment and Purification*, A. Bonilla-Petriciolet, D.I. Mendoza-Castillo, and H.E. Reynel-Ávila, Editors. 2017, Springer International Publishing: Cham. p. 109-138.

[13] Zahra, N., *Lead Removal from Water by Low Cost Adsorbents: A Review.* Pak. J. Anal. & Envir. Chem, 13 (2012) http://www.pjaec.pk/index.php/pjaec/article/view/198

[14] Yang, R., et al., *Thiol-modified cellulose nanofibrous composite membranes for chromium (VI) and lead (II) adsorption.* Poly, 55 (2014) 1167-1176. https://doi.org/10.1016/j.polymer.2014.01.043

[15] Suopajärvi, T., H. Liimatainen, M. Karjalainen, H. Upola, and J. Niinimäki, *Lead adsorption with sulfonated wheat pulp nanocelluloses.* J Water Process Eng, 5 (2015) 136-142. https://doi.org/10.1016/j.jwpe.2014.06.003

[16] Jin, X., Z. Xiang, Q. Liu, Y. Chen, and F. Lu, *Polyethyleneimine-bacterial cellulose bioadsorbent for effective removal of copper and lead ions from aqueous solution.* Bioresour. Technol., 244 (2017) 844-849. https://doi.org/10.1016/j.biortech.2017.08.072

[17] Ren, H., et al., *Efficient Pb(II) removal using sodium alginate–carboxymethyl cellulose gel beads: Preparation, characterization, and adsorption mechanism.* Carbohydr. Polym., 137 (2016) 402-409. https://doi.org/10.1016/j.carbpol.2015.11.002

[18] Shariatinia, Z. and A. Bagherpour, *Synthesis of zeolite NaY and its nanocomposites with chitosan as adsorbents for lead(II) removal from aqueous solution.* Powder Technol., 338 (2018) 744-763. https://doi.org/10.1016/j.powtec.2018.07.082

[19] Errea, M.I., E. Rossi, S.N. Goyanes, and N.B. D'Accorso, *Chitosan: From Organic Pollutants to High-Value Polymeric Materials*, in *Industrial Applications of Renewable Biomass Products*, S.N. Goyanes and N.B. D'Accorso, Editors. 2017, Springer. p. 251-264.

[20] Igberase, E. and P. Osifo, *Equilibrium, kinetic, thermodynamic and desorption studies of cadmium and lead by polyaniline grafted cross-linked chitosan beads from aqueous solution.* J Ind Eng Chem, 26 (2015) 340-347. https://doi.org/10.1016/j.jiec.2014.12.007

[21] Liu, B., et al., *Biosorption of lead from aqueous solutions by ion-imprinted tetraethylenepentamine modified chitosan beads.* Int. J. Biol. Macromol., 86 (2016) 562-569. https://doi.org/10.1016/j.ijbiomac.2016.01.100

[22] Jayakumar, R., M. Prabaharan, R.L. Reis, and J.F. Mano, *Graft copolymerized chitosan—present status and applications.* Carbohydr. Polym., 62 (2005) 142-158. https://doi.org/10.1016/j.carbpol.2005.07.017

[23] Varma, A.J., S.V. Deshpande, and J.F. Kennedy, *Metal complexation by chitosan and its derivatives: a review.* Carbohydr. Polym., 55 (2004) 77-93. https://doi.org/10.1016/j.carbpol.2003.08.005

[24] Ahmad, M., K. Manzoor, and S. Ikram, *Versatile nature of hetero-chitosan based derivatives as biodegradable adsorbent for heavy metal ions; a review.* Int. J. Biol. Macromol., 105 (2017) 190-203. https://doi.org/10.1016/j.ijbiomac.2017.07.008

[25] Hicks, R., A.K. Satti, G.D.H. Leach, and I.L. Naylor, *Characterization of toxicity involving haemorrhage and cardiovascular failure, caused by parenteral administration of a soluble polyacrylate in the rat.* J. Appl. Toxicol., 9 (1989) 191-198. 10.1002/jat.2550090310

[26] Bogdanffy, M.S., R. Sarangapani, D.R. Plowchalk, A. Jarabek, and M.E. Andersen, *A biologically based risk assessment for vinyl acetate-induced cancer and noncancer inhalation toxicity.* Toxicol. Sci., 51 (1999) 19-35. 10.1093/toxsci/51.1.19

[27] Tsao, C.T., et al., *Development of chitosan/dicarboxylic acid hydrogels as wound dressing materials.* J. Bioact. Compatible Polym., 26 (2011) 519-536. https://doi.org/10.1177/0883911511422627

[28] Valderruten, N., J.D. Valverde, F. Zuluaga, and E. Ruiz-Durántez, *Synthesis and characterization of chitosan hydrogels cross-linked with dicarboxylic acids.* React. Funct. Polym., 84 (2014) 21-28. https://doi.org/10.1016/j.reactfunctpolym.2014.08.006

[29] Kasaai, M.R., *Various Methods for Determination of the Degree of N-Acetylation of Chitin and Chitosan: A Review.* J. Agric. Food Chem., 57 (2009) 1667-1676. https://doi.org/10.1021/jf803001m

[30] Pujana, M.A., L. Perez-Alvarez, L.C.C. Iturbe, and I. Katime, *pH-sensitive chitosan-folate nanogels crosslinked with biocompatible dicarboxylic acids.* Eur. Polym. J., 61 (2014) 215-225. https://doi.org/10.1016/j.eurpolymj.2014.10.007

[31] Pujana, M.A., L. Pérez-Álvarez, L.C.C. Iturbe, and I. Katime, *Water dispersible pH-responsive chitosan nanogels modified with biocompatible crosslinking-agents.* Poly, 53 (2012) 3107-3116. https://doi.org/10.1016/j.polymer.2012.05.027

[32] Rinaudo, M., P. Le Dung, C. Gey, and M. Milas, *Substituent distribution on O, N-carboxymethylchitosans by 1H and 13C NMR.* Int. J. Biol. Macromol., 14 (1992) 122-128. https://doi.org/10.1016/S0141-8130(05)80001-7

[33] Yao, K., J. Li, F. Yao, and Y. Yin, *Chitosan-based hydrogels: functions and applications*. 2011: CRC Press.

[34] Jayakumar, R., et al., *Novel carboxymethyl derivatives of chitin and chitosan materials and their biomedical applications.* PrMS, 55 (2010) 675-709. https://doi.org/10.1016/j.pmatsci.2010.03.001

[35] Eckelt, A., J. Eckelt, and B. Wolf, *Solubility of Polymers*, in *Encyclopedia of Polymer Science and Technology*. 2011.

[36] Liu, J., et al., *Physical, mechanical and antioxidant properties of chitosan films grafted with different hydroxybenzoic acids.* Food Hydrocoll., 71 (2017) 176-186. https://doi.org/10.1016/j.foodhyd.2017.05.019

[37] Tran, H.T., et al., *Heavy metal biosorption from aqueous solutions by algae inhabiting rice paddies in Vietnam.* J. Environ. Chem. Eng., 4 (2016) 2529-2535. https://doi.org/10.1016/j.jece.2016.04.038

[38] Soulé, M.E.Z., F. Barraqué, F.M. Flores, R.M.T. Sánchez, and M.A. Fernández, *Carbon/montmorillonite hybrids with different activation methods: adsorption of norfloxacin.* Adsor, 25 (2019) 1361-1373. https://doi.org/10.1007/s10450-019-00098-2

[39] Vasiliu, S., I. Bunia, S. Racovita, and V. Neagu, *Adsorption of cefotaxime sodium salt on polymer coated ion exchange resin microparticles: Kinetics, equilibrium and*

thermodynamic studies. Carbohydr. Polym., 85 (2011) 376-387. https://doi.org/10.1016/j.carbpol.2011.02.039

[40] Inyinbor, A.A., F.A. Adekola, and G.A. Olatunji, *Kinetics, isotherms and thermodynamic modeling of liquid phase adsorption of Rhodamine B dye onto Raphia hookerie fruit epicarp.* Water Resour. Ind., 15 (2016) 14-27. https://doi.org/10.1016/j.wri.2016.06.001

[41] Dolphen, R., N. Sakkayawong, P. Thiravetyan, and W. Nakbanpote, *Adsorption of Reactive Red 141 from wastewater onto modified chitin.* J. Hazard. Mater., 145 (2007) 250-255. https://doi.org/10.1016/j.jhazmat.2006.11.026

[42] Mohammadzadeh Pakdel, P. and S.J. Peighambardoust, *Review on recent progress in chitosan-based hydrogels for wastewater treatment application.* Carbohydr. Polym., 201 (2018) 264-279. https://doi.org/10.1016/j.carbpol.2018.08.070

[43] Hopkins, D. and K. Hawboldt, *Biochar for the removal of metals from solution: A review of lignocellulosic and novel marine feedstocks.* J. Environ. Chem. Eng., 8 (2020) 103975. https://doi.org/10.1016/j.jece.2020.103975

[44] Deng, L., Y. Su, H. Su, X. Wang, and X. Zhu, *Sorption and desorption of lead (II) from wastewater by green algae Cladophora fascicularis.* J. Hazard. Mater., 143 (2007) 220-225. https://doi.org/10.1016/j.jhazmat.2006.09.009

[45] Ayuba, S., A.A. Mohammadib, M. Yousefic, and F. Changanic, *Performance evaluation of agro-based adsorbents for the removal of cadmium from wastewater.* Desalination Water Treat., 142 (2019) 293-299. https://doi.org/10.5004/dwt.2019.23455

[46] Khan, N.A., et al., *Performance evaluation of column-SBR in paper and pulp wastewater treatment: optimization and bio-kinetics.* Desalin. Water Treat., 156 (2019) 204-219. 10.5004/dwt.2019.23775

[47] Liu, Y., *Is the free energy change of adsorption correctly calculated?* J. Chem. Eng. Data, 54 (2009) 1981-1985. https://doi.org/10.1021/je800661q

[48] Lima, E.C., A. Hosseini-Bandegharaei, J.C. Moreno-Piraján, and I. Anastopoulos, *A critical review of the estimation of the thermodynamic parameters on adsorption*

equilibria. Wrong use of equilibrium constant in the Van't Hoof equation for calculation of thermodynamic parameters of adsorption. J. Mol. Liq., 273 (2019) 425-434. https://doi.org/10.1016/j.molliq.2018.10.048

[49] Arencibia, A., M.S. López-Gutiérrez, and J.M. Arsuaga, *Efficient aqueous As(III) removal by adsorption on thiol-functionalized mesoporous silica*. J. Chem. Technol. Biotechnol., n/a (2020) https://doi.org/10.1002/jctb.6339

[50] Heydari Moghaddam, M., et al., *Performance investigation of Zeolitic Imidazolate Framework – 8 (ZIF-8) in the removal of trichloroethylene from aqueous solutions.* Microchem. J., 150 (2019) 104185. https://doi.org/10.1016/j.microc.2019.104185

[51] Sharifi, S., et al., *Modeling and optimizing parameters affecting hexavalent chromium adsorption from aqueous solutions using Ti-XAD7 nanocomposite: RSM-CCD approach, kinetic, and isotherm studies.* J. Environ. Health Sci. Eng., 17 (2019) 873-888. 10.1007/s40201-019-00405-7